October 2017

Grid-Based RFID Indoor Localization Using Tag Read Count and Received Signal Strength Measurements

Nanda Gopal Jeevarathnam
University of South Florida, nandagopal@mail.usf.edu

Grid-Based RFID Indoor Localization Using Tag Read Count and Received Signal Strength Measurements

by

Nanda Gopal Jeevarathnam

A thesis submitted in partial fulfillment
of the requirements for the degree of
Master of Science in Electrical Engineering
Department of Electrical Engineering
College of Engineering
University of South Florida

Major Professor: Ismail Uysal, Ph.D.
Jing Wang, Ph.D.
Nasir Ghani, Ph.D.

Date of Approval:
October 24, 2017

Keywords: Artificial Neural Network, Lateration, LOS Channel, Maximum Likelihood Estimation, On-Off Keying, Regression

DEDICATION

I dedicate this work to my parents and to Professor Dr. Ismail Uysal.

ACKNOWLEDGMENTS

I would like to thank Professor Dr.Ismail Uysal for all the guidance and advice throughout my study. Dr.Ismail Uysal gave me the opportunity to explore RFID technology and its applications in great depth.

Thank you, Arundhoti Ferdous, senior member of my lab and RFID research team for all the help and support in completing this study. I also like to thank Samuel Mercier for his help with the function implementation in Matlab.

I would like to thank all my friends for their support, especially Ravikiran Shivarajaiah and Praveen Durai, who built up confidence and motivation in myself.

A special thanks to my committee members Dr. Jing Wang and Dr. Nasir Ghani for their motivation and patience. Finally, I would like to thank my parents and family members for their support throughout my life.

TABLE OF CONTENTS

LIST OF TABLES

LIST OF FIGURES

ABSTRACT

Passive ultra-high frequency (UHF) radio frequency identification (RFID) systems have gained immense popularity in recent years for their wide-scale industrial applications in inventory tracking and management. In this study, we explore the potential of passive RFID systems for indoor localization by developing a grid-based experimental framework using two standard and easily measurable performance metrics: received signal strength indicator (RSSI) and tag read count (TRC). We create scenarios imitating real life challenges such as placing metal objects and other RFID tags in two different read fields (symmetric and asymmetric) to analyze their impacts on location accuracy. We study the prediction potential of RSSI and TRC both independently and collaboratively. In the end, we demonstrate that both signal metrics can be used for localization with sufficient accuracy whereas the best performance is obtained when both metrics are used together for prediction on an artificial neural network especially for more challenging scenarios. Experimental results show an average error of as low as 0.286 (where consecutive grid distance is defined as unity) which satisfies the grid-based localization benchmark of less than 0.5.

CHAPTER 1: INTRODUCTION

1.1 Localization

In recent years, location-based services(LBSs) have gained importance due to groundbreaking advances in wireless devices and technologies. These services improve the convenience of human life in places such as industrial warehouses, libraries, hospitals, smart homes and other places where quick and accurate localization of objects is of main concern [1].

In the literature, numerous solutions using Cellular-network, Computer Vision, Ultrasound, Infrared Ray, Bluetooth, RFID and so on have been proposed for indoor positioning. This work focuses on indoor localization in industrial warehouse using passive RFID systems which are considered dominant. Indoor localization involves tracking of objects, vehicles, or people within a building or enclosed infrastructure. The main warehouse activities include receiving, transfer, order picking, calibration, order sorting and shipping [2]. In applications involving supply chain management, inventory control and monitoring of the objects in the warehouse is critical. The numerous objects in the warehouse are referred to as pallets. Position information of pallets is beneficial to perform the above tasks. Henceforth, each objects needs to been monitored carefully every now and then to ensure efficient operation of the warehouse.

For order picking, pallet position information can efficiently reduce the distance of travel and location response time. Likewise, the decision of order routing demands the exact position of each pallet. This also helps in removing the faulty objects and sorting the objects in the warehouse in real-time. The receiving activity includes unloading products and moving them into the

warehouse. Although information is recorded when products go in or out of the warehouse, there is ample opportunity for errors to occur which demands the need for developing a reliable localization system. This work presents a novel RFID localization approach using two easily obtainable system performance metrics: tag read count(TRC) and received signal strength indicator(RSSI).

1.2 Indoor Localization

Indoor localization is generally used for tracking and monitoring objects (e.g., track objects in shopping centers or in big warehouses), navigating individuals to a point of interest (e.g., entry/exit point in the building), or even in advanced games that depend on the current location context. In addition, there are other potential scenarios for such kind of localization systems in industrial environments [3]. For instance, maintenance employees who are responsible for multiple large industry halls could use the location for a context-aware system to effortlessly locate and navigate in an industrial environment. It can help them discover and maintain machines, turbines, or other industry equipment. In addition, it could give live information for real-time tracking of the nearby engines, turbines, outlets, or other equipment's [4][5].

In the literature, it is stated frequently that localization in an industrial environment confronts additional challenges causing deviations (scattering, diffraction or reflection) in the radio frequency (RF) signal. This is because of the large number of active and passive paths of the RF signal. Active paths include electromagnetic radiations by other industrial equipments such as engines, vents, and panels, and by the equipments using the same frequency range. Passive paths can emerge mainly through metallic and nonmetallic walls or objects absorbing signals that results in shadowing effects or by metallic objects such as metallic meshes and pipes that reflect and diffuse signals which creates multipath transmission [6]. The people working in the indoor

environment can also cause passive paths. To achieve indoor localization, we can use any of the common identification technologies such as GPS, Bluetooth, Wi-Fi and RFID depending on the nature of the environment.

1.3 Outdoor Localization

Outdoor Localization is extremely crucial in applications such as road vehicular tracking, distance education, disaster management, battlefield, marine biology and warehouse management. Some of the outdoor localization techniques capable of tracking large number of objects are Global Positioning System (GPS), cellular-based, Wi-Fi technology and RFID technology [7]. The GPS Localization System, which is commonly used for outdoor localization suffers from high power consumption and high cost since it has to localize hundreds of objects present in the environment. The accuracy of GPS system is in the range of few meters depending on the application. Localization using mobile technology measures received signal strength indicator (RSSI), which is the measure of the power present in a received radio signal. The base transceiver stations (BTS) communicates the value of the RSSI to the mobile terminal which has the location information. The architecture of a time difference of arrival based localization system for GSM mobile terminals provides localization accuracy of 5 meters [8]. Outdoor localization using Wi-Fi access points with specific IDs provides a mean error of few meters based on the level of received signals and number of neighbors. The active RFID positioning systems provides outdoor localization by combining relevant information, such as received signal strength indicator (RSSI), round-trip time-of-flight (TOF), time-difference of arrival (TDOA), or phase difference-of-arrival (PDOA) of the RFID signals.

CHAPTER 2: LOCALIZATION TECHNIQUES

Various geolocation technologies can be utilized to estimate client (person or object) geographical position. The large diversification of prevailing wireless technologies and the growing number of wireless enabled devices triggered the widespread use of Location Based Services (LBS). The measurement of Radio Frequency signals in indoor environment is difficult to achieve as it is subjected to numerous problems such as extreme multipath, erratic line-of-sight (LOS) path, absorption, diffraction, and reflection. Henceforth, location systems consist of three main phases to counter these effects. In the following sections, we discuss the different measurement techniques, Position computation methods and localization algorithms which are required for indoor localization.

2.1 Measurement Techniques

The objects in the indoor environment needs to be tracked every now and then. This phase is responsible for measuring the physical quantity of the object with which the object can be localized [9]. Different techniques can be used for this purpose, such as Received Signal Strength (RSS), Time of Arrival (TOA), Time Difference of Arrival (TDOA), Phase difference of arrival (PDOA), or Proximity [1] [10] [11] [12].

2.1.1 TOA

The propagation time of a radio signal is proportional to the distance between a reference point such as a single transmitter to the target such as a remotely based server or receiver. For 2-D positioning, TOA signal measurements must be obtained from at least three reference points, as

shown in Figure 2.1 with a technique called triangulation. The one-way propagation time is measured, and the distance between the two points is calculated. The distance 'd' between a pair of nodes can be obtained by using measurements of signal propagation delay or time of flight (τ_p) calculated as follows.

$$\tau_p = \frac{d}{c}$$

where, c is the speed of electromagnetic waves in air (c=3 x 10^8 m/s).

In Figure 2.1, node A transmits a packet to node B. Node B transmitts an acknowledgement packet after a known or measured response delay (τ_d). After receiving the acknowledgment, node A estimates the signal round-trip time (τ_{RT}) as per the below equation.

$$\tau_{RT} = 2\tau_p + \tau_d$$

Knowing the value of signal round-trip time, node A then calculates the actual distance between the two nodes. This procedure is repeated at all the nodes and the intersection of the measured distance of all the three nodes denotes the position.

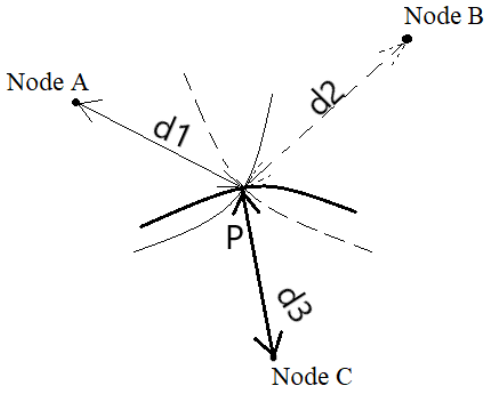

Figure 2.1 Positioning based on TOA measurements.

For proper estimation using direct TOA, the below mentioned criterias must be employed in the system. First, all transmitters and receivers in the system have to be precisely synchronized.

Second, a timestamp must be labeled in the transmitting signal in order for the measuring unit to discern the distance the signal has traveled.

2.1.2 TDOA

In TDOA technique, the relative location of a transmitter is calculated by using the difference in time at which the signal emitted by a target arrives at single or multiple measuring units called as the receivers. TDOA can be calculated by any of the two methods described below. In the first method multiple signals are broadcasted from synchronized transmitters and the receiver measures the TDOA. In the second method a reference signal is broadcasted by receiver and is received by several fixed transmitters. The prerequisite for both the method is that the transmitters are firmly synchronized through a network. A 2-D target location can be estimated from the two intersections of two or more TDOA measurements, as shown in Figure 2.2.

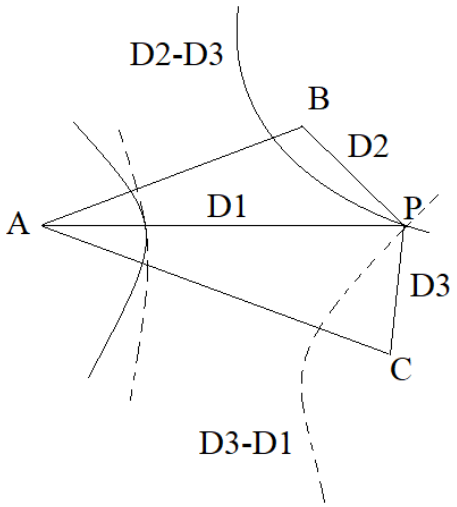

Figure 2.2 Positioning based on TDOA measurements.

The Figure 2.2 consists of three fixed receivers giving two TDOAs and thus provide an intersection point which is the estimated location of the target. This method requires a precise time reference between the measuring units. Like TOA, TDOA has few drawbacks. In indoor

environments, a LOS channel is rarely available. Moreover, radio propagation often suffers from multipath effects thus affecting the time of flight of the signals.

2.1.3 RSS

The RSS measurement is mainly based on the principle that greater the distance between two nodes, the weaker the strength of the received signal.The previously discussed two schemes have some drawbacks. For indoor environments, it is difficult to find a LOS channel between the transmitter and the receiver. Radio propagation in such environments would suffer from multipath effect. The time and angle of an arrival signal would be affected by the multipath effect; thus, the accuracy of estimated location could be decreased. An alternative approach is signal attenuation-based methods which attempts to calculate the signal path loss due to propagation. Theoretical and empirical models are used to translate the difference between the transmitted signal strength and the received signal strength into a range estimate, as shown in Figure 2.3.

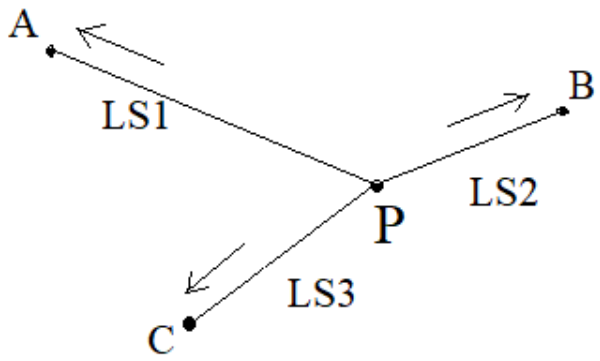

Figure 2.3 Positioning based on RSS measurements.

In the Figure, LS1,LS2 and LS3 are values of the received signal strengths of signals received at Nodes A,B and C respectively. Due to severe multipath fading and shadowing present in the indoor environment, path-loss models do not always hold. The parameters employed in these models are site-specific. The accuracy of this method can be improved by utilizing the premeasured

RSS contours centered at the receiver [12] or by taking multiple measurements at several base stations.

2.1.4 PDOA

The Phase-difference-of-arrival method uses the carrier phase (or phase difference) to estimate the distance of the target as shown in the Figure 2.4. This method is also called phase of arrival (POA) or received signal phase (RSP)[12]. It requires transmitters placed at particular locations and assumes that they emit pure sinusoidal signals with frequency f, with zero phase offset for calculation of the phases of signals received at a target point. A finite transit delay should be maintained for the signal transmitting from each transmitter to the receiver.The disadvantage of the RSP method with respect to the indoor environments is that it strongly needs a LOS signal path to mimimize localization errors.

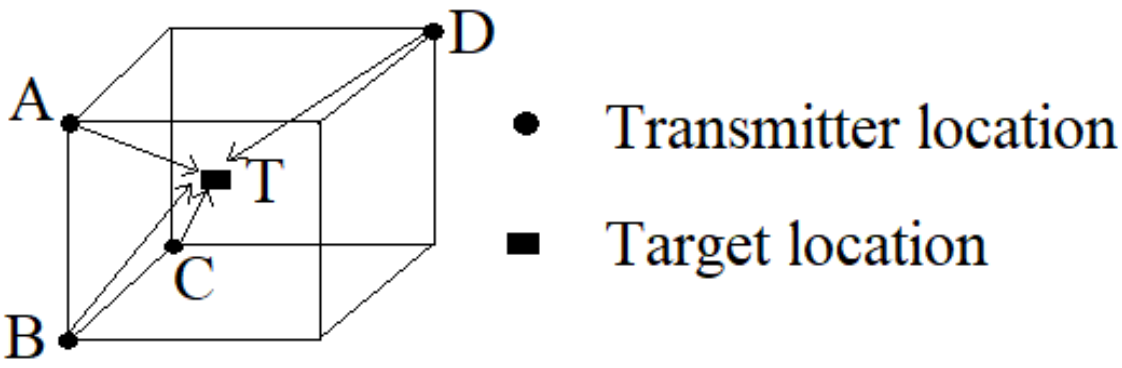

Figure 2.4 Positioning based on phase of signal.

2.1.5 Proximity

Proximity approach relies on dense deployment of antennas. The target is located when it enters in the radio range of a single antenna, each having a well-known position. When a mobile target is detected by a single antenna, it is considered to be co-located with it. When more than one antenna detects the mobile target, it is considered to be co-located with the one that receives

the strongest signal. This method is relatively simple to implement. However, the accuracy depends on the size and number of the cells.

2.2 Methods for Position Computation

This component is responsible for computing the position of a node based on available information about the estimated distance from previous signal measurements and the position of reference points. Recognized techniques used in this component include triangulation, trilateration, and multilateration [14]. These three algorithms have unique advantages and disadvantages for the particular chosen applications or services. Hence, using more than one type of positioning algorithms at the same time could result in better performance. In order to alleviate the measurement errors, traditional triangulation with positioning algorithms such as scene analysis or proximity is developed.

2.2.1 Triangulation

This technique estimates the direction of the nodes, as in angle of arrival(AoA) systems [15]. The node positions are determined with the help of the trigonometry laws of sines and cosines and properties of triangles to estimate the target's location. The triangulation approach, illustrated in Figure 2.5, consists of measuring the angle of incidence (or Angle of Arrival - AOA) of at least two reference points. The estimated position corresponds to the intersection of the lines defined by the angles.

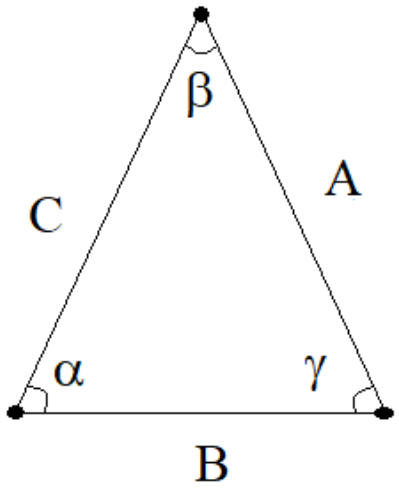

Figure 2.5 Triangulation technique.

2.2.2 Trilateration

This technique determines the position of a node from the intersection of three circles of the three anchor nodes. The radius of each circle corresponds to the measured distance at that particular node as shown in Figure 2.6 below. The intersection point 'P' is the estimated point. However, in an irrational environment, the distance measurement is not perfect; hence, more than three nodes are required to achieve localization.

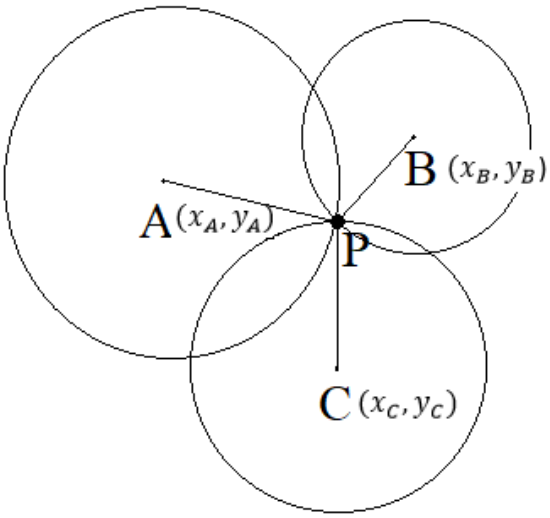

Figure 2.6 Trilateration technique.

2.2.3 Multilateration

Trilateration technique cannot accurately estimate the position of a node if the distance measurements are noisy. A possible solution is to use multilateration technique or also known as Maximum Likelihood (ML) estimation, which determines distance measurements at multiple neighbor nodes to localize as shown in Figure 2.7 below. By this method we can achieve a more accurate estimated distance compared to Trilateration technique since there are more neighbor nodes [15]. It is not easy to model the radio propagation in the indoor environment because of severe multipath, low probability for availability of line-of sight (LOS) path, and specific site parameters such as floor layout, moving objects, and numerous reflecting surfaces. In such cases, we can use an alternative measurement metrics such as received signal strength Indicator (RSSI) or tag read count (TRC) to improve the accuracy.

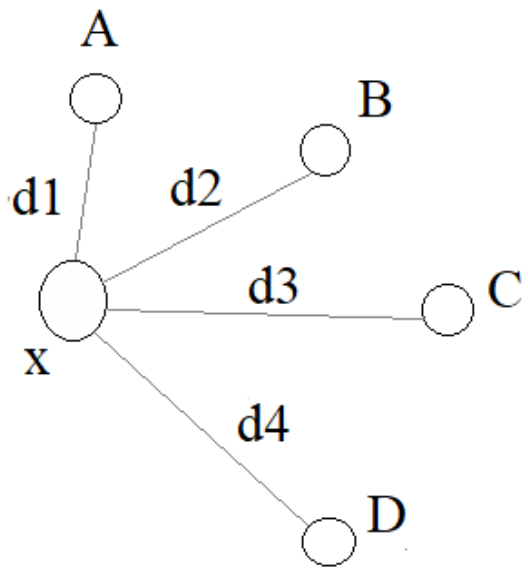

Figure 2.7 Multilateration technique.

2.3 Localization Algorithm

This is the main component of a localization system which determines how the available information will be manipulated in order to estimate the target's position. The performance of any localization algorithm depends on a number of factors, such as number of anchor nodes, node density, computation and communication costs, algorithm accuracy and so on [14]. All approaches have their own advantages and disadvantages, making them feasible for different applications. We discuss proximity based localization algorithms below. This type of algorithm uses location fingerprinting technique to localize the object [16]. Location fingerprinting refers to techniques that match the fingerprint of some characteristic of a signal that is location dependent. The algorithm first collects the features (fingerprints) of an area and then estimates the location of an object by matching measurements with the nearest priori location fingerprints. RSS-based location fingerprinting is commonly used for indoor localization. There are two phases for location fingerprinting: offline phase and online or run-time phase. During the offline phase, a site survey of the environment is achieved. The location coordinates/labels and respective signal strengths from nearby base stations/measuring units are collected. During the online phase, a location positioning technique uses the currently observed signal strengths and previously collected information to figure out an estimated location. This model provides inaccurate estimation in cases where there is deviation in the measurement of the fingerprints caused as a result of diffraction, reflection, and scattering in the indoor environments. The location fingerprinting-based positioning algorithms use pattern recognition techniques such as probabilistic methods, k-nearest-neighbor (kNN), Artificial Neural Networks (ANN), support vector machine (SVM), and smallest M-vertex polygon (SMP) [7][8]. The section below discusses Probabilistic Models, k-nearest-neighbor (kNN) and Artificial Neural Networks (ANN).

2.3.1 Probabilistic Models

Common pattern recognition algorithms are probabilistic in nature which use statistical inference to find the accurate location for a given object [17]. Unlike other algorithms, which simply provides the best output, probabilistic algorithms also output a probability of the object in the estimated location. In addition, many probabilistic algorithms provide a list of the N-best locations with associated probabilities, for some value of N, instead of simply a single best location. When the number of possible locations is very small as in the case of classification algorithms, N may be set so that the probability of all possible locations is considered. Probabilistic algorithms have many advantages over non-probabilistic algorithms:

• They provide a confidence value associated with their choice.

• They can discard an output when the confidence of choosing this particular output is too low.

• Probabilistic pattern-recognition algorithms can be more successfully incorporated into larger machine-learning tasks to avoid the problem of error propagation by considering the output probabilities.

Bayesian-network-based and/or tracking-assisted positioning techniques are used for location-aware and location-sensitive applications which involves realistically significant issues like calibration, active learning, error estimation, and tracking with history.

2.3.2 K-nearest Neighbor (kNN)

In pattern recognition, the *k*-nearest neighbors algorithm (*k*-NN) is a non-parametric method used for classification and regression[18]. The kNN algorithm uses the collected data to search for k closest matches of known locations in signal space from the previously-built database [19]. The matching is performed based on the principle of root mean square (RMS) errors. The two types of kNN that can be used to estimate the location of the object

are weighted kNN, where averaging the k location values is achieved with adopting the distances in signal space as weights and unweighted kNN, where averaging the k location values is achieved without adopting the distances in signal space. In this algorithm, k is the parameter adapted for better performance.

2.3.3 Neural Networks

Neural network or 'artificial' neural network (ANN), is a computing system made up of a number of simple, highly interconnected processing elements, which process information by their dynamic state response to external inputs [20]. Neural networks comprise of layers. Layers consists of a numerous interconnected 'nodes' which contain an 'activation function'. Patterns that are fed to the network via the 'input layer' communicates to one or more 'hidden layers' where the desired processing is done by means of a system of weighted 'connections'. The graphic representation of the neural network is shown in Figure 2.8 below.

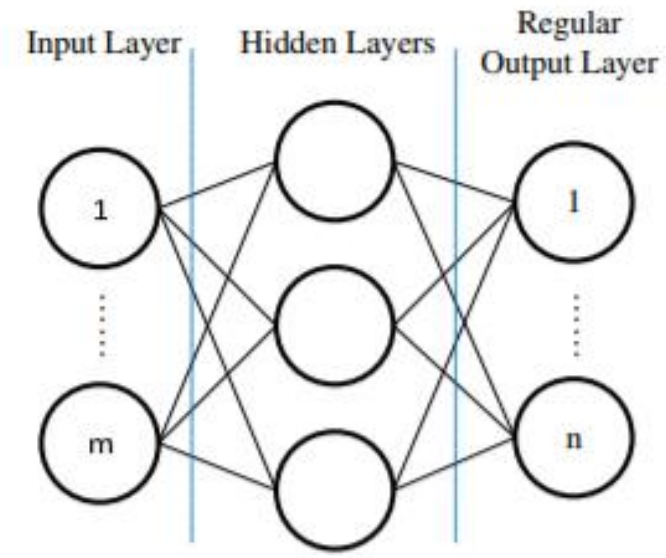

Figure 2.8 Graphic view of the basic Neural Network.

Most of the ANNs have some form of 'learning rule' which modifies the weights of the connections considering the fed-in input patterns. Although there are many different kinds of learning rules used by neural networks, the delta rule is often utilized by the most common class of ANNs called 'backpropagation neural networks' (BPNNs). Here, backpropagation refers to the backwards propagation of error. After the training phase of the neural network, the remaining input samples can be analyzed. To achieve this, the neural network runs in forward propagation mode. In the forward propagation mode, the new inputs are processed by the middle layers just as in training phase, however, at this point the output is preserved with no backpropagation. At the last stage, an output layer compiles propagated activations of the hidden layers to generate a decision which can be used for further analysis and interpretation.

.

CHAPTER 3: WIRELESS-BASED POSITIONING SYSTEMS

3.1 GPS

Global positioning system (GPS) is one of the most commonly used positioning systems in outdoor environments [21]. GPS signals are quite weak, and they can even be blocked to some extent by the roof and walls of the building. In addition, GPS can only be implemented in places where line-of-sight is available for the satellite signals. Hence, poor coverage of satellite signal for indoor environments decreases its accuracy and makes it unsuitable for indoor localization. GPS indoors technique provides an accuracy of about 5–50m in most indoor environments.

3.2 WLAN

The wireless local area network (WLAN) operating in 2.4 GHz Industrial, Scientific and Medical (ISM) band has become very popular in public places. This technology has a bit rate of 11, 54, or 108 Mbps and a range of 50–100 m. WLAN can be combined with a location server for indoor localization. The accuracy of typical WLAN positioning systems using RSS measurements is approximately 3 to 30 m, with an update rate of few seconds.

3.3 Bluetooth

Bluetooth operates in the 2.4-GHz Industrial, Scientific and Medical (ISM) band. It provides a gross bit rate of 1 Mbps and an approximate range of 10–15 m. Bluetooth is highly ubiquitous being embedded in most phones, personal digital assistants (PDAs), etc. Bluetooth tags are nothing but small transceivers where every Bluetooth device has a unique ID. This ID is used for locating the Bluetooth tag using three major types of units: positioning server(s), wireless

access points, and wireless tags.. This technology provides an accuracy of around 2m with the positioning delay of 15 to 30 seconds.

3.4 Cellular Networks

For the estimation of location of outdoor mobile users, a number of systems have used global system of mobile/code division multiple access (GSM/CDMA) mobile cellular network. However, this technology cannot be used for indoor tracking systems to estimate the location of indoor mobile clients since the accuracy of the method is generally low in the range of 50–200m depending on the cell size. Indoor positioning based on mobile cellular network is possible if the received RSS is strong. The received RSS depends on the base station covering the building. Accurate GSM-based indoor localization is possible with larger base stations which provide good RSS values. It is also observed that the accuracy is higher in densely covered areas such as urban places compared to the rural environments due to presence of large number of base stations.

3.5 Ultra-Wide Band Technology

This technology is rapidly growing for its suitability in the indoor environment [1] [22]. In UWB, an active RFID tag transmits signals as a computer calculates the position of the tag with the estimation algorithms such as Time of arrival(TOA) or time difference of arrival (TDOA) and so on. UWB technology provides good accuracy as the computed estimation is easy with minimal errors. Therefore, UWB is viewed as a promising technology in Indoor positioning. UWB operates by sending ultrashort pulses of typically less than 1 ns, with a low duty cycle of typically 1: 1000. On the spectral domain, the system has a wide band ranging larger than 500 MHz. Localization with UWB technology has the following advantages. UWB transmits a signal over multiple bands of frequencies simultaneously from 3.1 GHz to 10.6 GHz which is better than conventional RFID systems which operate on single bands of the radio spectrum.

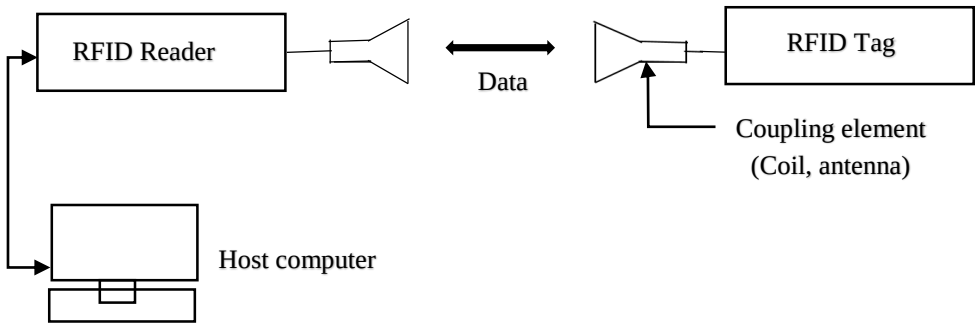

Figure 3.1 Communication of basic RFID System.

UWB tags can operate across a broad area of the radio spectrum with consuming less power than conventional RF tags. UWB short duration pulses are easy to filter thereby rejecting multipath signals. The UWB signal passes easily through walls, equipment and clothing and provides minimal interference in metallic and liquid environments. With exploiting the characteristics of time synchronization of UWB communication, very high indoor location accuracy of 20 cm can be achieved. However, UWB systems are not as widespread as passive RFID systems for a number of reasons. First if all, the up-front implementation costs for UWB systems are very high. In addition to that, UWB uses active tags for communication which are more expensive and also require consistent maintenance for batter upkeep.

3.6 Near-Field Technology

This technology is based on near field electromagnetic ranging (NFER) that uses low frequency up to 1 MHz and long wavelength of 300 m. This technology uses the deterministic relationship that exists between angle formed by the magnetic field and electric field of the received signal. The operating distance is usually less than 10 centimeters with NFC technology. The main problem with this technology is its high cost to achieve localization due to the use of large antennas.

CHAPTER 4: RFID LOCALIZATION SYSTEM – 1

Passive RFID readers uses the electromagnetic backscatter to communicate with the tags. An RFID tag gets activated when the continuous wave signal is incident on its antenna. The tags reply by modulating the backscatter wave using on-off keying (OOK) technique. In this experiment, we investigate the localization potential of a passive RFID system on a grid-based setup where the read field is divided into 6 locations and a passive tag can be placed in any one of these locations. We use the Ultra High Frequency (860-960 MHz) band for this indoor localization application [13]. This section briefly describes the localization system setup, conditions at which the data is collected and the proposed localization algorithm.

4.1 System Description

The system consists of two main components: ATID AB700 UHF RFID handheld reader and a UPM Frog 3D RFID tag. This localization system is setup similarly to available localization systems in the literature [22] [23]. We utilized the handheld Reader for capturing tag read count (TRC) information. The handheld reader that works on EPC Global Class 1 Gen 2 protocol has an internal circularly polarized antenna. The operating frequencies of the handheld reader are in the range of 900 MHz to 928 MHz, which is the legal UHF band in the United States. The passive RFID tag is of size 5 cm x 5 cm and is attached to a box of dimensions 23 cm x 23 cm x 23 cm for this experiment.

The size of the testing area on the laboratory floor used for the experiments is chosen as 0.96 square meters (a rectangular region of 1.2 x 0.8 sq. m.). We use traditional grid-based

approach to localize the tags. The testing area is divided into a 3x2 rectangular grid comprising of six cells. The size of each cell is 0.4 x 0.4 sq. m. The handheld reader was set-up along the diagonals of the grid. The experimental set-up is shown in the Figure 4.1 below.

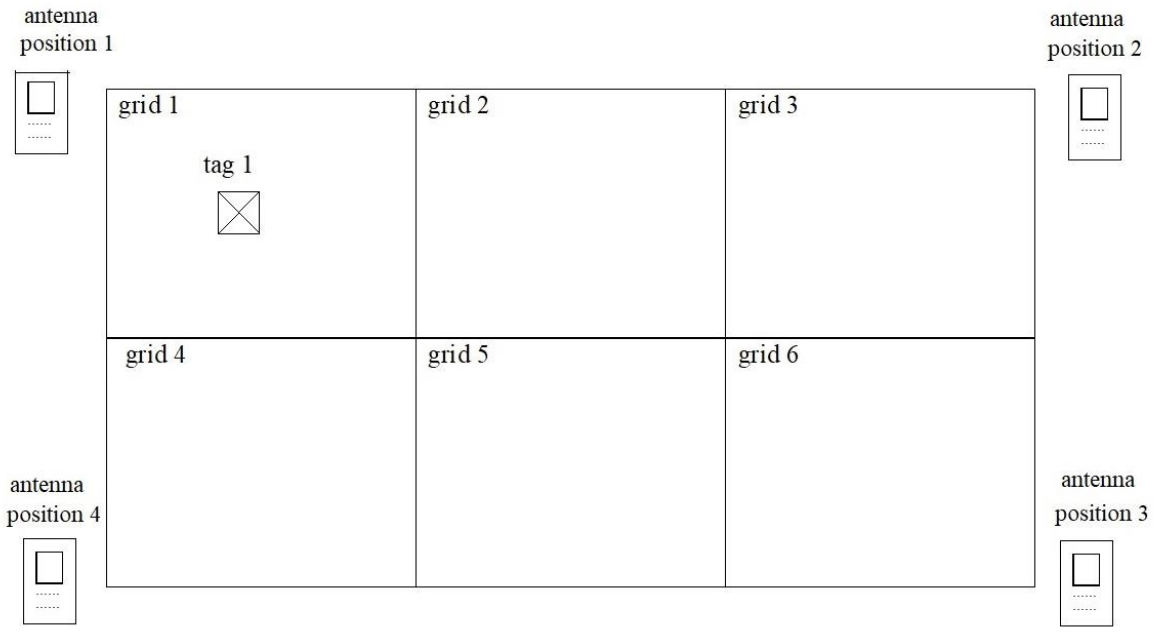

Figure 4.1 RFID Localization System-1 setup.

4.2 Data Collection Phase

As mentioned above, the RFID tag is attached to one of the outer sides of the box. The output power level of the RFID handheld reader is set to 27 dBm which is equal to 0.5 Watts except for metal phase where the power level used is 24 dBm which is equal to 0.25 Watts. The height of the RFID handheld reader is set to 0.4 meters. The time period for phase 1 at which each TRC value is collected is set to 10 seconds, whereas for all the remaining phases, TRC values are collected for two time periods of 5 and 10 seconds. Figure 4.2 shows picture of the handheld reader.

Figure 4.2 A photo of the RFID handheld reader.

4.2.1 Phase 1: Orientation

For each grid location, the TRC values were collected by the antennas placed at the four corners of the grid. Therefore, we get four TRC values for each position of the tag in the grid. The TRC values were collected with respect to all the six possible orientations of the RFID tag- top, bottom and four sides of the box. The overall data collection procedure of the RFID localization system is as shown in the Figure 4.3 below.

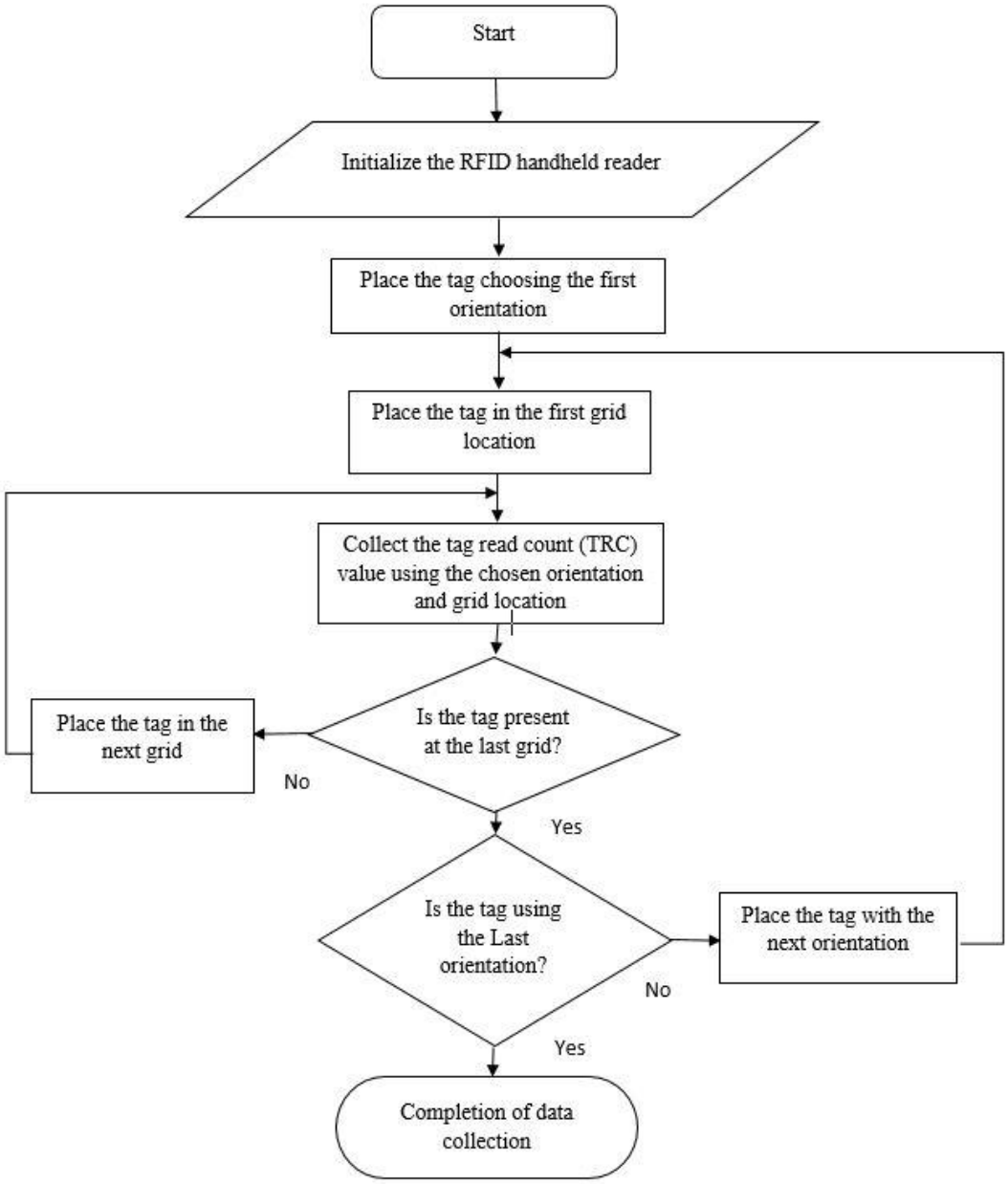

Figure 4.3 Flowchart showing the operation of the RFID Localization System-1 setup.

This procedure is repeated for all the six grid locations of the tagged object resulting in a total of 6 (orientation) x 6 (grid locations) x 4 (antenna positons) = 144 measurements. In addition, the power level is changed to 24 dBm which is equal to 0.25 Watts for one of the orientation (tag facing upwards) resulting in 6 grid locations x 4 antenna positions = 24 measurements. Lastly, the

height of the antenna is changed to one meter keeping the same orientation (tag facing upwards) resulting in 6 grid locations x 4 antenna positions = 24 measurements. Hence this phase results in a total of 144+24+24=192 measurements. The RFID tag used in the localization system is shown in Figure 4.4.

Figure 4.4 A photo of the RFID tag attached to the box.

4.2.2 Phase 2: Metal

In this case, a metal object of dimensions 20 cm x 20 cm is introduced to the rectangular grid. In this phase, the orientation of the tag is fixed and its attached to the box facing upwards as in the previous phase as shown in Figure 4.5. By keeping the same orientation of the tag we can observe the effect of the metal on the TRC [24]. Initially, the metal object and RFID tag is placed in the first grid location. The effect of the metal object on the RFID tag can be found by observing the TRC values for all the grid locations of the tag and antenna positions resulting in 1 (TRC) x 6 (grid locations) x 4 (antenna positions) = 24 measurements. Next, the same procedure is repeated by all the six grid locations of the metal object resulting in 6 x 24 = 144 measurements. This

procedure is used to collect TRC for two time periods (5s and 10s) resulting in a total measurement count of 288. Figure 4.6 shows the photograph of the metal piece used for this phase.

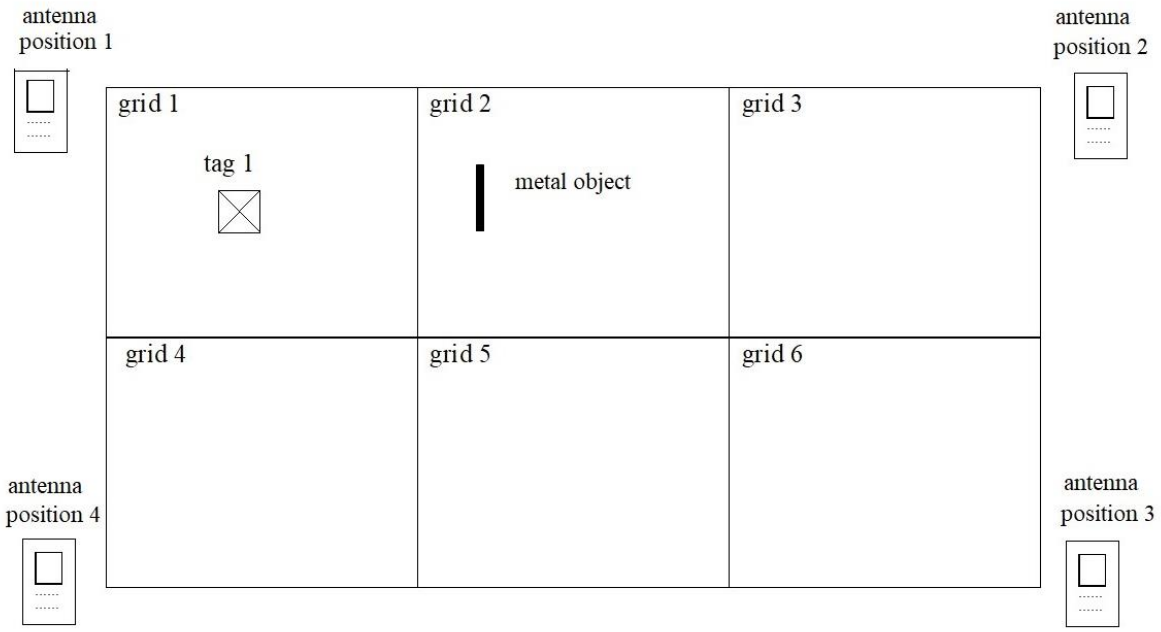

Figure 4.5 RFID Localization System-1 setup with metal piece.

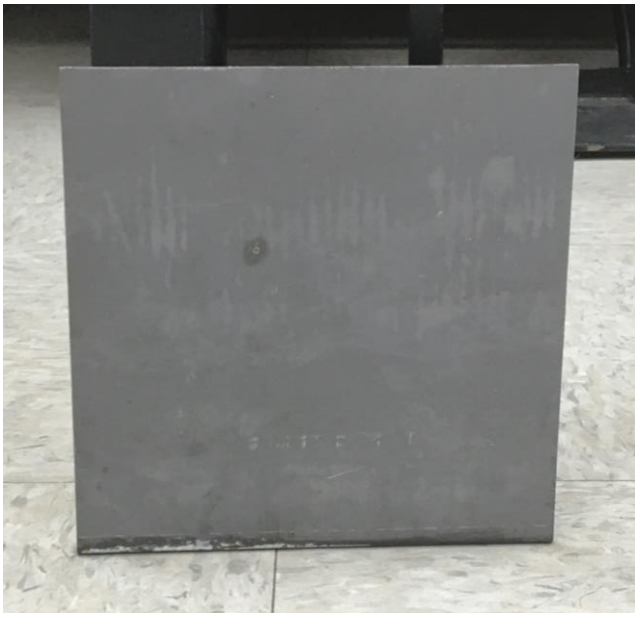

Figure 4.6 A photo of the metal piece.

4.2.3 Phase 3: One Additional Tag

In this phase, an additional RFID tag is introduced to the rectangular grid and the effect is observed as shown in Figure 4.7. This additional tag is attached to the side of a second object such that they can be moved separately within the grid. The photograph of the added RFID tag is shown in Figure 4.8. Both RFID tags are initially present at the first grid location and the TRC is captured for the primary RFID tag. Just like the previous metal case, the primary RFID tag is moved to all the grid locations keeping the added RFID tag constant at the first grid location for all the four antenna positions resulting in 6 x 4 =24 measurements. The same procedure is repeated until the additional tag is placed in all the six grid locations resulting in a total number of 24 x 4 = 144 measurements. This procedure is used to collect TRC for two time periods (5s and 10s) resulting in a total measurement count of 288.

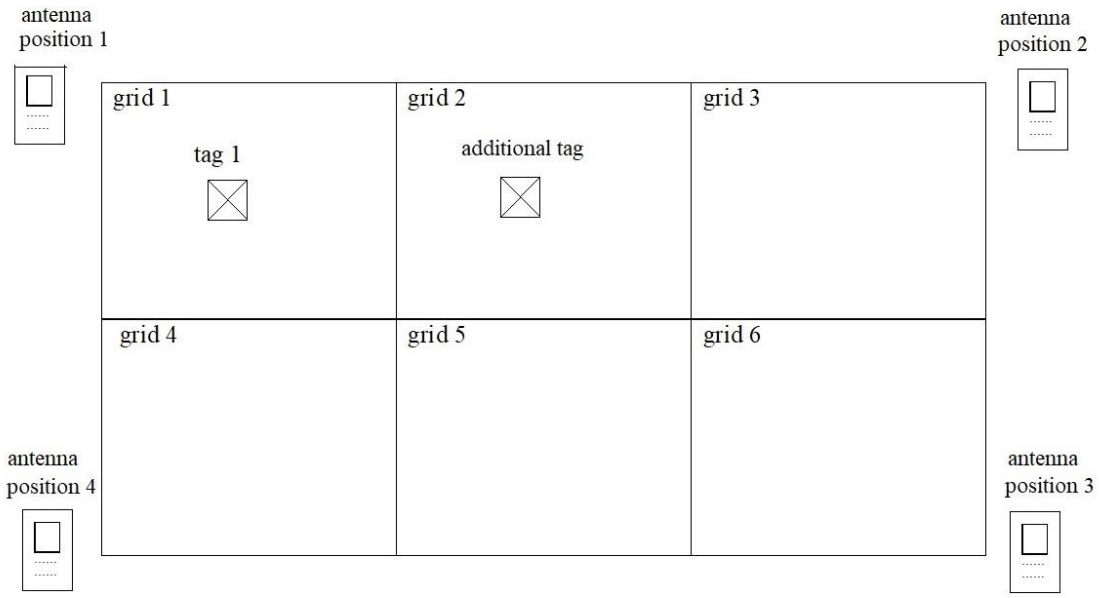

Figure 4.7 RFID Localization System-1 with one additional tag.

Figure 4.8 A photo of the additional RFID tag.

4.2.4 Phase 4: Two Additional Tags

This setup is exactly the same as one additional tag setup except two additional tags are attached to one side of the second object and they are moved together as TRC values are collected resulting in the same number of 288 measurements. The system setup and photograph of the two RFID tags are shown in Figure 4.9 and Figure 4.10 respectively.

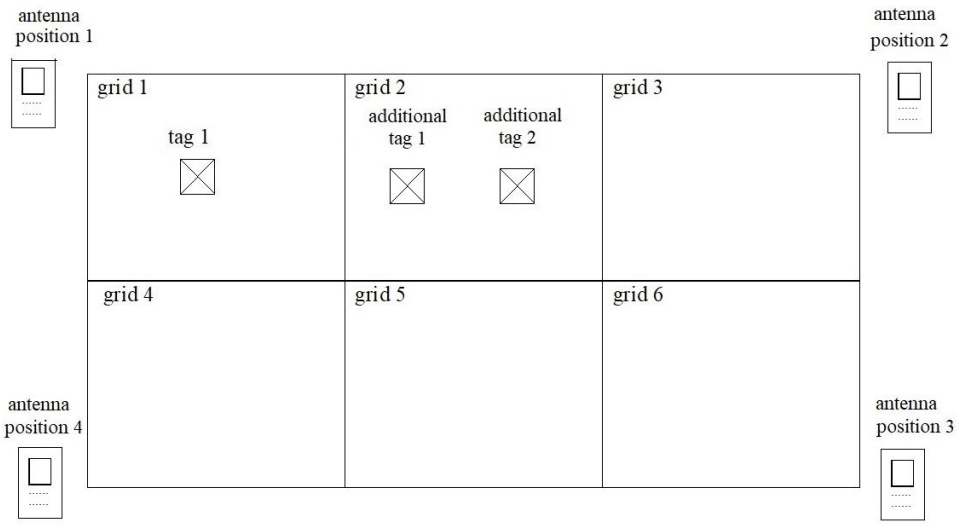

Figure 4.9 RFID Localization System-1 setup with two additional tags.

Figure 4.10 A photo of the two additional RFID tags.

4.3 Neural Network

An Artificial Neural Network (ANN) is an information processing prototype that is built with inspiration from our biological nervous systems such as the brain [25]. The main component of this prototype is the unique structure of the information processing system which comprises of a large number of highly interconnected processing elements called neurons working in agreement to solve specific problems. An ANN operates in three main phases: training phase, testing phase and validation phase. An ANN can be configured for a specific application such as pattern recognition or data classification during the training phase when the connections between neurons and their relative weights are adjusted depending on the input data samples.

4.3.1 Data Processing Phase

The obtained TRC from the experimental measurements as described in the previous section are fed into the ANN (Artificial Neural network) in Matlab as shown in Figure 4.11. The experimental data collected from the four phases (single tag/metal object/additional tag/two

additional tags) are fed into the neural network in stages. Initially, 192 samples of TRC values obtained from the first phase is fed into the neural network. Six-fold cross-validation technique is used to validate the algorithm as follows. Out of the 192 samples, in six-fold cross validation the collected data samples are divided into six partitions. The training/testing of the network is repeated six times, using a different partition for testing each time the network is trained. In this approach 4/6th of the samples are set aside for training the algorithm, 1/6th is set aside for early-stopping to prevent the algorithm from overfitting and 1/6th is set aside for testing and validating the algorithm. Using the data samples, the neural network learns to identify the grid location of the tag during the training phase. To estimate to error in the identified location, the distance between the adjacent grid locations is assumed as unity and the relative distance between each grid location is computed to generate a distance matrix of dimensions 6x6 where D(i,j) corresponds to the scaled distance between grid numbers i and j.

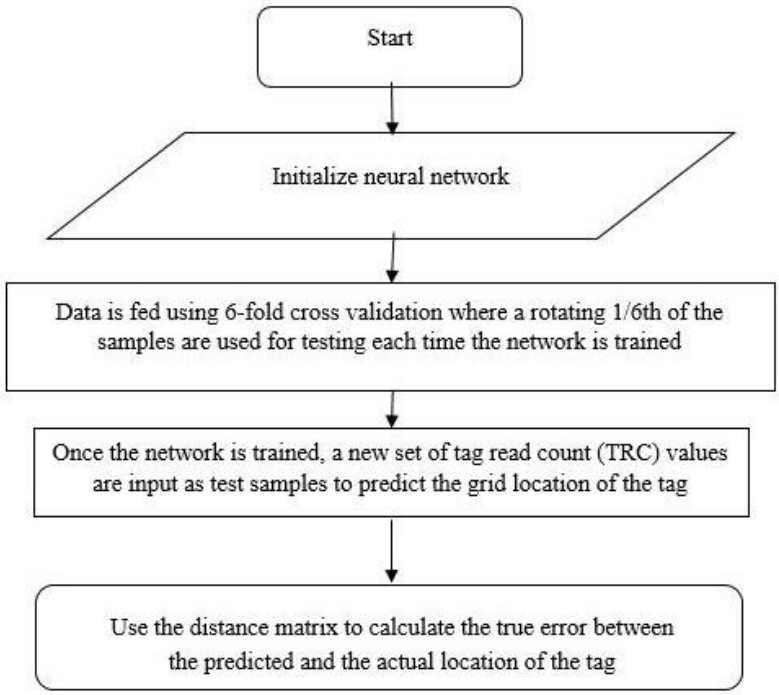

Figure 4.11 Flowchart showing the operation of the Neural Network.

In the second stage, additional TRC values obtained from the metal phase is added to the existing dataset which then goes through the same six-fold cross-validation training/testing process. In the third and fourth stages of data augmentation, additional TRC values from one and two additional tag phases of the experiment is added to the dataset for subsequent six-fold cross-validation process.

4.4 Results and Discussion

Table 4.1 Location accuracy results using different neural network topologies / augmented datasets and scenarios. Each scenario corresponds to a different phase of data collection process where: S1 - single tag with different orientations/antenna heights/power, S2 - single tag with metal object, S3 - one additional tag on the grid and S4 - two additional tags on the grid.

Hidden layer size	Samples	Total samples	Experiment	fold-1 error	fold-2 error	fold-3 error	fold-4 error	fold-5 error	fold-6 error	Average Error
5 5	192 (48 x 4)	192 (48 x 4)	S1	0.9268	1.0303	1.0303	0.6768	1.5081	0.9563	1.02143333
	288 (72 x 4)	480 (120 x 4)	S2	0.5207	0.7328	0.5207	0.15	0.25	0.4207	0.43248333
	288 (72 x 4)	768 (192 x 4)	S3	0.8609	0.5333	0.3567	0.2942	1.0504	1.006	0.68358333
	288 (72 x 4)	1056 (264 x 4)	S4	0.6568	0.4318	0.4601	0.5149	0.9362	0.761	0.6268
10 10	192 (48 x 4)	192 (48 x 4)	S1	0.375	0.6036	0.8536	0.5518	0.8018	0.4268	0.6021
	288 (72 x 4)	480 (120 x 4)	S2	0.5828	0.8121	0.35	0.15	0.4	0.35	0.44081666
	288 (72 x 4)	768 (192 x 4)	S3	0.5571	0.4192	0.1875	0.5	0.6379	0.5571	0.47646666
	288 (72 x 4)	1056 (264 x 4)	S4	0.6567	0.4091	0.6458	0.4373	0.5737	0.67	0.56543333
5	192 (48 x 4)	192 (48 x 4)	S1	0.7286	0.8313	1.1036	0.8018	0.8536	0.6768	0.83261666
	288 (72 x 4)	480 (120 x 4)	S2	0.6828	0.8121	0.4	0.15	0.3207	0.25	0.43593333
	288 (72 x 4)	768 (192 x 4)	S3	0.5388	0.5203	0.2942	0.4192	0.7652	0.596	0.52228333
	288 (72 x 4)	1056 (264 x 4)	S4	0.6472	0.4412	0.4867	0.4734	0.5696	0.737	0.55918333

Table 4.1(Continued)

10	192 (48 x 4)	192 (48 x 4)	S1	0.7286	0.5518	0.7286	0.5518	0.9786	0.7286	0.711333333
	288 (72 x 4)	480 (120 x 4)	S2	0.5621	0.6914	0.3	0.2	0.4707	0.3707	0.432483333
	288 (72 x 4)	768 (192 x 4)	S3	0.6272	0.5516	0.2813	0.375	0.6768	0.7339	0.540966667
	288 (72 x 4)	1056 (264 x 4)	S4	0.7223	0.3182	0.4318	0.551	0.5925	0.6058	0.536933333
20	192 (48 x 4)	192 (48 x 4)	S1	0.6768	0.5518	0.7803	0.6768	0.9786	1.2581	0.8204
	288 (72 x 4)	480 (120 x 4)	S2	0.7328	0.7414	0.7414	0.15	0.4	0.5707	0.55605
	288 (72 x 4)	768 (192 x 4)	S3	0.7286	0.3696	0.2188	0.375	0.583	0.6531	0.488016667
	288 (72 x 4)	1056 (264 x 4)	S4	0.5604	0.3182	0.4185	0.5149	0.5391	0.6848	0.505983333

The results presented in the Table 4.1 shows that TRC can reasonably localize an RFID tag in a rectangular grid of 1.2 x 0.8 sq. m with six locations. Most of the common experimental scenarios that the RFID tag can be exposed are considered in this experiment. A total combined number of 1056 samples were collected from all the above scenarios. The selection of hidden layer size is important to get accurate results [26]. The optimal size of the hidden layer is recommended to be usually between the size of the input and size of the output layers and generally provides decent performance when the number of hidden layers equals one or the number of neurons is the mean of the number of neurons in the input and output layers. Hence, we evaluated a selection of hidden layer sizes around these commonly accepted numbers such as [5 5], [10 10], 5, 10 and 20 provided the results for each of these selections for a final comparison. An average error of 0.5059 was achieved for the network with hidden layer size of 20 neurons when using all the data samples collected in the experiment using six-fold cross-validation. This distance error is satisfactory considering the fact that a single grid distance was taken as unity (1) which means an error of approximately 0.5 corresponds to the “correct-localization-within-grid” benchmark.

CHAPTER 5: RFID LOCALIZATION SYSTEM – 2

Although TRC can be used as a reliable metric for grid localization as seen from the results in chapter 4, RFID readers can collect other signal information from the read field, one of which is the received signal strength indicator (RSSI). In this chapter, we describe a second experiment where we measure both RSSI and TRC values in a similar grid-based localization framework. We localize the tag using TRC and RSSI both separately and collaboratively using three experimental phases: single tag, metal object and two additional tags. The system performance for all the three cases is observed. The details about the experimental system setup, hardware and data processing systems are discussed in the sections below.

5.1 System Description

The localization system in this setup comprises of four main components; Motorola FX7400 fixed RFID reader, UPM Frog 3D RFID tag, Motorola ANT-71720-01 RFID Antenna and the control unit (PC). The fixed RFID reader which is suitable for retail inventory and asset management provides tag processing in real time for EPC Class1 Gen2 compliant RFID tags. The reader is connected to the RFID Antenna using a copper cable of length equal to 2 meters throughout this experiment. The RFID Reader is a 4- Port device, i.e., four RFID antennas can be connected at a given time which captures both RSSI and TRC values at a given time. In our experiment, we used a single antenna. RFID Antenna is reliable for both indoor environments (warehouse) as well as outdoor environments (docking zone). It is resistant to extreme heat and cold, making it applicable to any application. The antenna which is right hand circularly polarized,

operates in the UHF Band (900MHz to 928 MHz) and provides a gain of 6 dBi. The UPM Frog 3D RFID tag used in this localization system is the same tag as in the previous localization system and is attached to a box of dimensions 23 cm x 23 cm x 23 cm as before.

Experiments are conducted on the lab floor as in the previous localization system. Unlike the first experiment which uses an asymmetrical grid (2x3), this experiment utilizes a slightly larger grid with a symmetrical setup (3x3) which occupies 1.44 square meters (a square region of 1.2 x 1.2 sq. m.). Traditional grid-based approach is utilized to localize the tags. The testing area is divided into a 3x3 square grid comprising of nine cells. The size of each cell is 0.4 x 0.4 sq. m which is the same as localization system-1. The RFID antenna is placed along the diagonals of the grid to obtain the measurements. The experimental set-up is shown in the figure below.

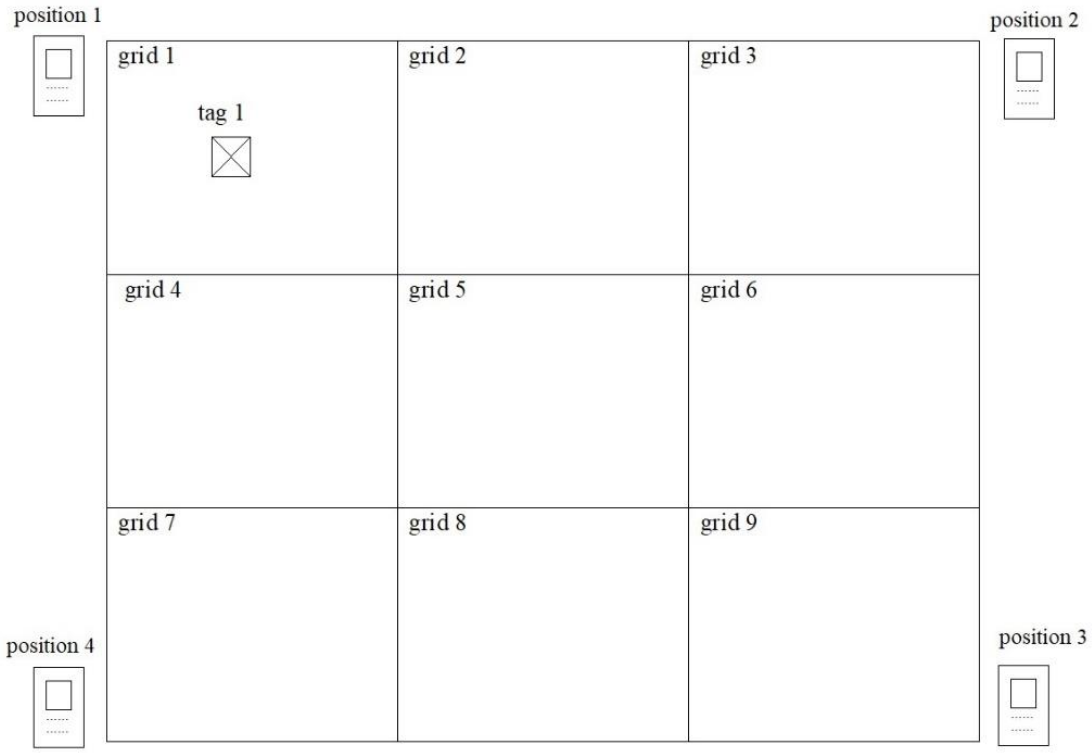

Figure 5.1 RFID Localization System-2 setup.

5.2 Data Collection Phase

The RFID tag is attached to the side of the box. The power level of the fixed RFID reader as shown in Figure 5.2 is set to 30 dBm which is equal to 1 Watt. The fixed RFID reader is placed vertically to the ground. The time period at which each TRC value is collected is 5 seconds. In this localization system, there are three phases of data collection. One additional tag phase of RFID localization system-1 is neglected here since the obtained localization accuracies from localization sysem-1 for one and two additional tag phases were almost identical. A photo of the RFID antenna used to collect the data is shown in Figure 5.3.

Figure 5.2 A photo of fixed RFID reader.

Figure 5.3 A photo showing the front side and back side of the RFID antenna.

5.2.1 Phase 1: Orientation

For each grid location, the TRC and RSSI values are collected by antennas placed at the four corners of the grid as shown in the Figure 5.4. Therefore, we get four TRC and RSSI values for each position of the tag in the grid with respect to all the six possible orientations of the RFID tag. The overall data collection procedure of the RFID localization system is as shown in the flowchart below. This procedure is repeated for all the six grid locations of the metal object resulting in 2 (RSSI + TRC) x 9 (cells) x 6 (orientations) x 4 (antenna positions) = 432 measurements.

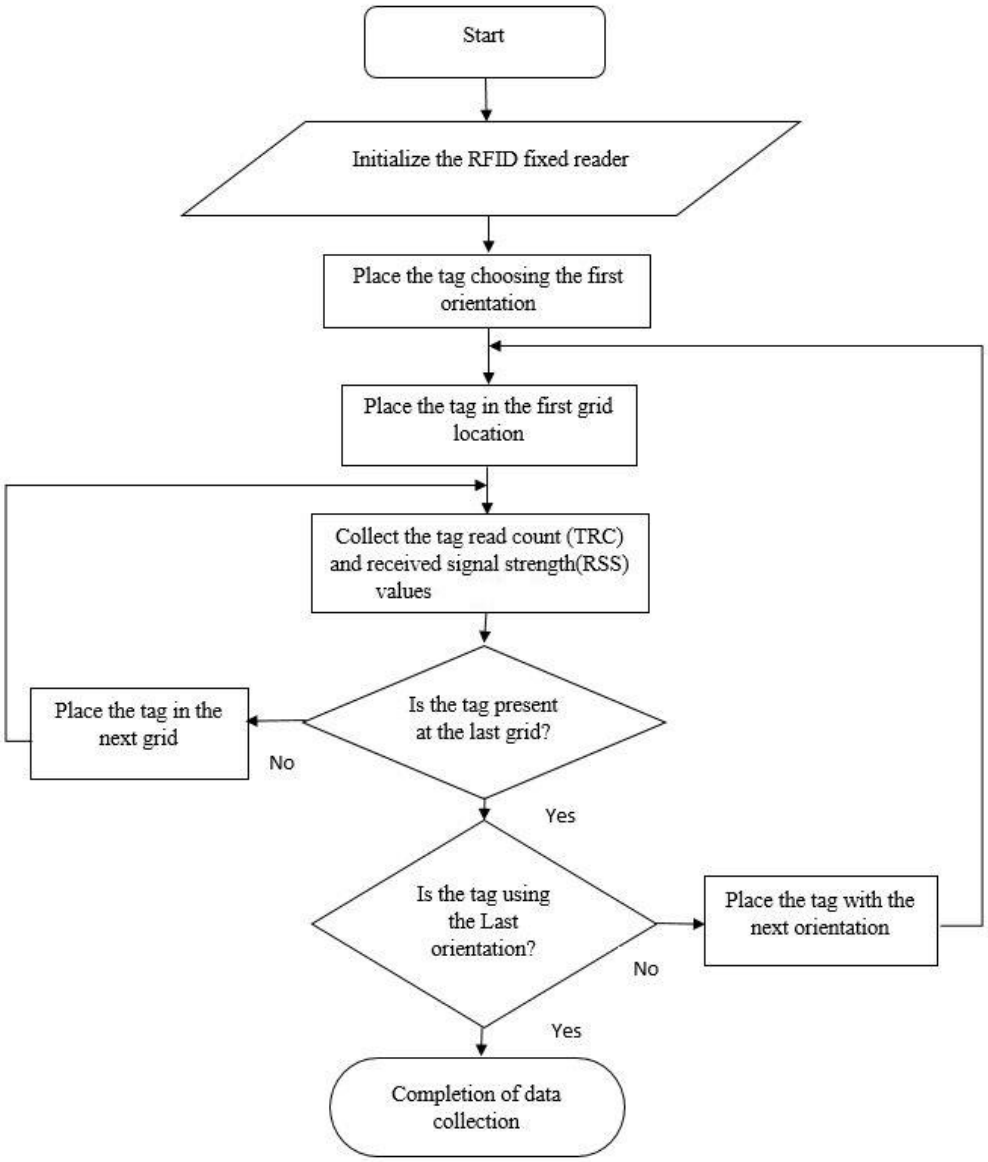

Figure 5.4 Flowchart showing the operation of the RFID Localization System-2 setup.

5.2.2 Phase 2: Metal

This phase is the same as RFID localization system-1 except that both the TRC and RSSI values are captured. The experimental setup is shown in Figure 5.5. The resulting measurements from this phase is 2 (RSSI + TRC) x 9 (metal positions) x 9 (grid locations) x 4 (antenna positions) = 648.

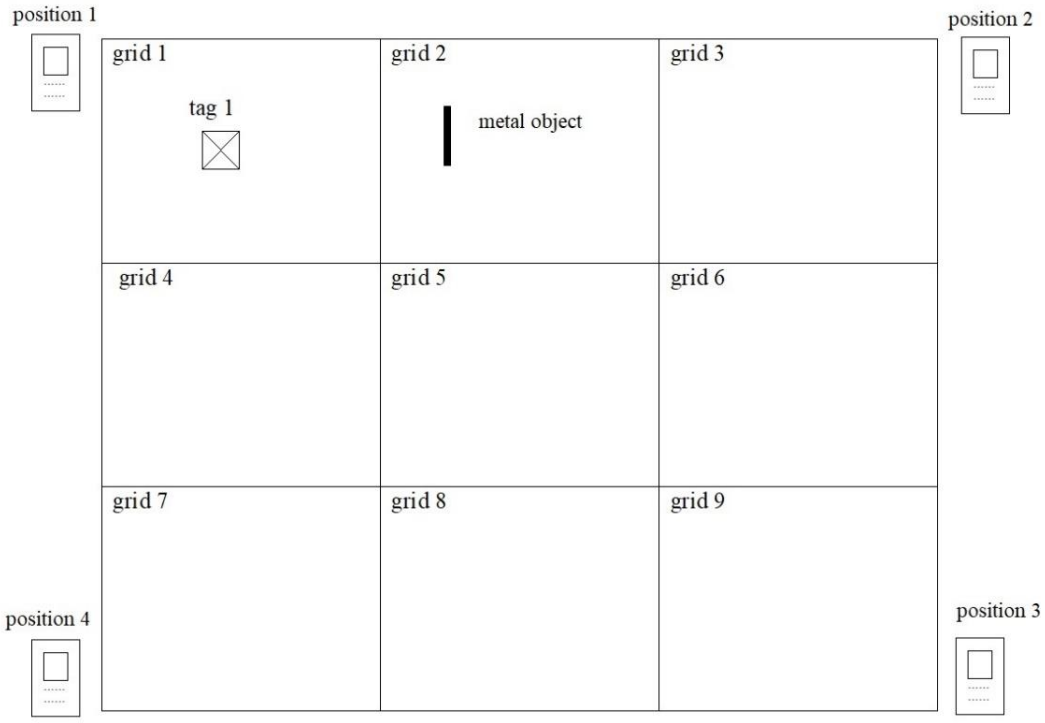

Figure 5.5 RFID Localization System-2 setup with metal piece.

5.2.3 Phase 3: Two Additional Tags

This operation of this phase is the same as RFID localization system-1. The same procedure is repeated until the additional tag is placed in all the six grid locations. The experimental setup is shown in Figure 5.6. A total number of 2 (RSSI + TRC) x 9 (additional tag positions) x 9 (grid locations) x 4 (antenna positions) = 648 measurements were collected in this phase.

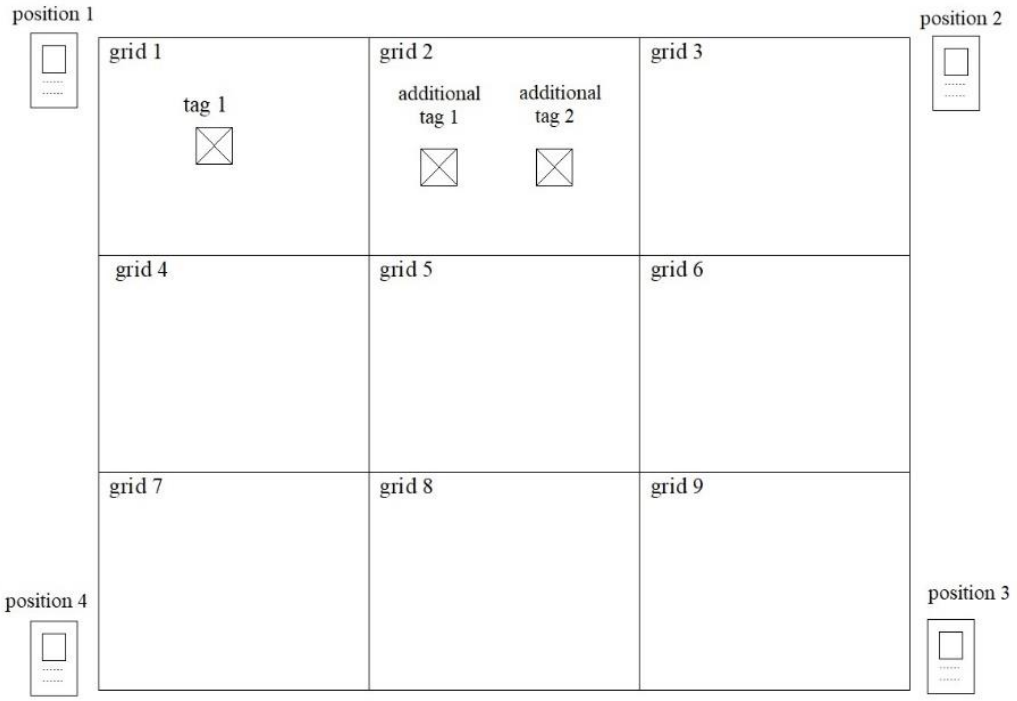

Figure 5.6 RFID Localization System-2 setup with two additional tags.

5.3 Data Processing Phase

Fixed RFID reader along with the antenna is used to collect the TRC and RSSI values. To control the reader, a USB cable is connected between the reader and personal computer (control unit). The necessary software is also installed in the personal computer. RFID fixed reader is connected to the personal computer using the IP address of the RFID reader. The screenshot in Figure 5.7 shows the connected RFID reader detecting the RFID tag with EPC: 000000000000000000011BAD. We can also see the TRC and RSSI readings for a run time of about 5 seconds. For each trail, the average value of the RSSI reading is computed.

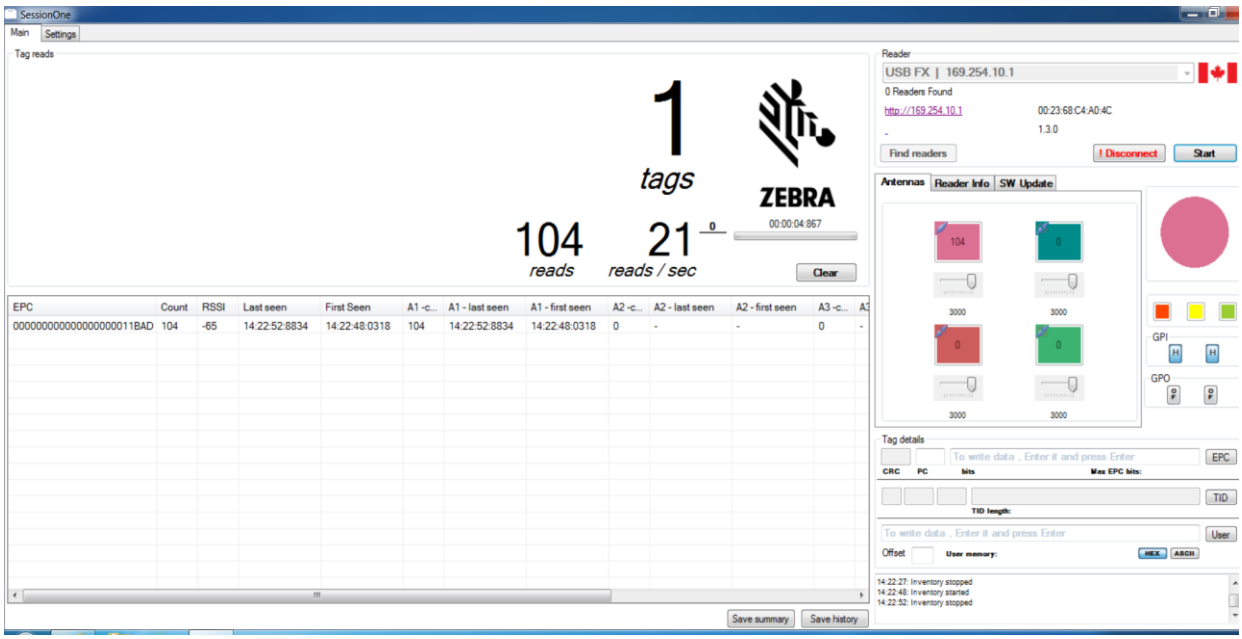

Figure 5.7 Screenshot of the captured TRC and RSSI with the fixed RFID reader.

The obtained TRC and RSSI values from the experimental measurements as described in the previous section are fed into the ANN in Matlab and the operation is as shown in Figure 5.7.

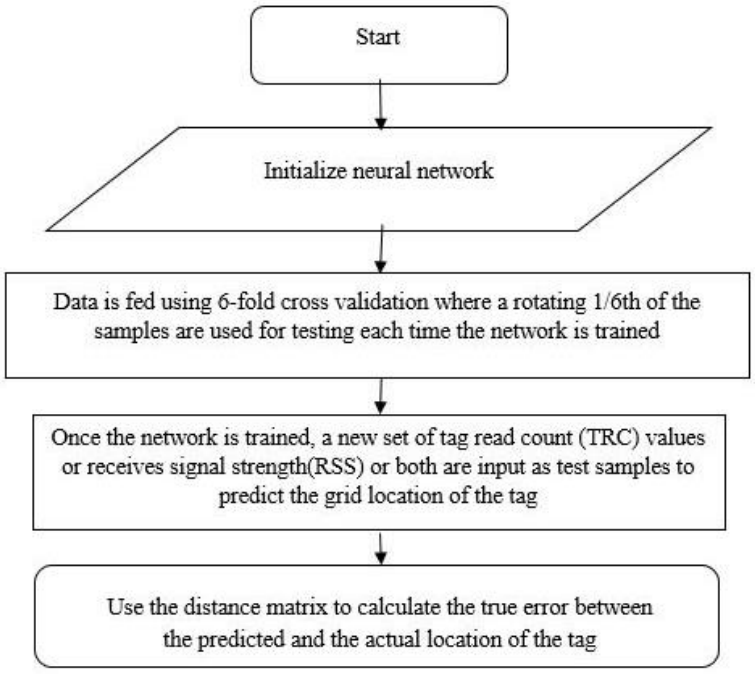

Figure 5.8 Flowchart showing the operation of the Neural Network.

The experimental data collected from the three phases (single tag/metal object/two additional tags) are fed into the neural network in stages. Initially, 432 samples of TRC values obtained from the first phase is fed into the neural network. Six-fold cross-validation technique is used to validate the algorithm as follows. A total of 432 collected data samples are divided into six partitions using six-fold cross validation technique as in RFID localization system-1. The training/testing phase is also the same as RFID localization system-1. To estimate to error in the identified location, the distance between the adjacent grid locations is assumed as unity and the relative distance between each grid location is computed to generate a distance matrix of dimensions 9x9 where D(i,j) corresponds to the scaled distance between grid numbers i and j. Figure 5.9 shows the relative distance computation with respect to tag at grid location 1.

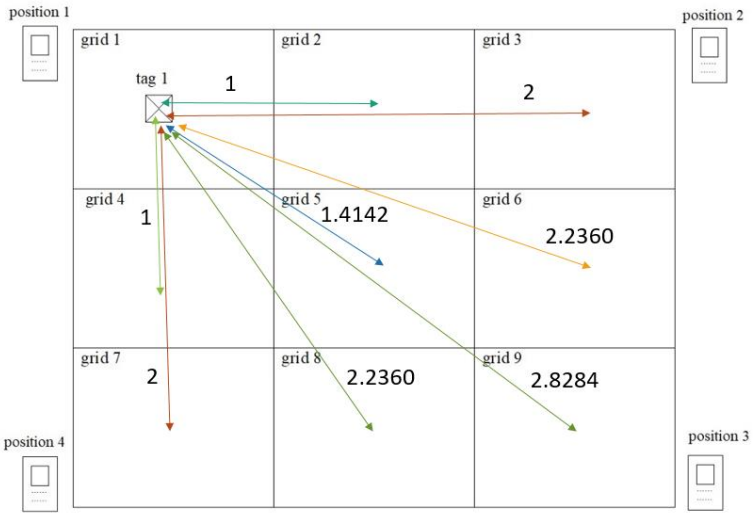

Figure 5.9 Figure showing the relative distances with respect to tag at grid location 1.

In the second stage, additional TRC and RSSI values obtained from metal phase is added to the existing dataset which then goes through the same six-fold cross-validation training/testing process. In the third stage of data augmentation, additional TRC and RSSI values from two additional tag phases is added to the dataset for subsequent six-fold cross-validation process.

5.4 Results and Discussion

5.4.1 Using Tag Read Count(TRC)

The results presented in the below table are obtained by using the TRC values only. The values of the hidden layer size are chosen the same as the first experiment as the data dimensions are approximately the same. The algorithm is run 100 times for all six folds for highest statistical significance. The last column describes the overall average error which is the averaged over all six folds. It can be concluded that the localization is possible for the selected square grid of 1.2 x 1.2 sq. m with nine locations.

Table 5.1 Location accuracy results using TRC for different neural network topologies / augmented datasets and scenarios. Each scenario corresponds to a different phase of data collection process where: S1 - single tag with different orientations/antenna heights/power, S2 - single tag with metal object, and S3 - one additional tag on the grid.

Hidden layer size	Samples	Total samples	Experiment	fold-1 error	fold-2 error	fold-3 error	fold-4 error	fold-5 error	fold-6 error	Average Error
[5 5]	216	216(54 x 4)	S1: TRC	1.4488	1.3521	1.3736	1.4383	1.4106	1.433	1.4094
	324	540 (135 x 4)	S2: TRC	1.0756	1.4397	1.6326	1.6176	1.8521	1.6931	1.551783333
	324	864 (216 x 4)	S3: TRC	1.1183	1.3667	0.6016	0.6278	1.1643	1.393	1.045283333
[10 10]	216	216(54 x 4)	S1: TRC	1.4332	1.3455	1.3818	1.425	1.425	1.4403	1.408466667
	324	540 (135 x 4)	S2: TRC	0.9492	1.4002	1.649	1.5554	1.9099	1.7257	1.531566667
	324	864 (216 x 4)	S3: TRC	1.2103	1.2754	0.6667	0.3794	0.6278	1.8508	1.001733333
5	216	216(54 x 4)	S1: TRC	1.3556	1.3038	1.3962	1.4247	1.4336	1.4099	1.3873
	324	540 (135 x 4)	S2: TRC	0.9772	1.4104	1.6672	1.5355	1.9203	1.7256	1.539366667
	324	864 (216 x 4)	S4: TRC	0.6278	1.4516	0.3596	0.3794	0.7191	1.439	0.829416667
10	216	216(54 x 4)	S1: TRC	1.3982	1.3024	1.3644	1.3822	1.3975	1.4017	1.3744
	324	540 (135 x 4)	S2: TRC	0.9001	1.4285	1.6298	1.499	1.927	1.7646	1.524833333
	324	864 (216 x 4)	S4: TRC	1.073	1.4976	0.5167	0.3143	0.5818	0.85	0.805566667
20	216	216(54 x 4)	S1: TRC	1.3896	1.329	1.3054	1.4456	1.3976	1.4137	1.38015
	324	540 (135 x 4)	S2: TRC	0.8958	1.4289	1.6075	1.4898	1.9435	1.775	1.523416667
	324	864 (216 x 4)	S4: TRC	0.8302	1.3469	0.7389	0.4254	0.6278	1.0072	0.8294

From the table, it can be observed that minimum error of 0.8294 is achieved for a hidden layer size of 20 neurons considering the data collected from all the phases. The error values in table 5.1 are significantly higher than the ones reported in table 4.1. The best localization performance is obtained with a hidden layer size of 20 neurons when cumulative dataset is used. The error in this case is 0.83 compared to 0.51 obtained in table 4.1. There could be various reasons for this discrepancy but the biggest impact is the change in grid size. Whereas in the previous system a grid size of 2x3 was used in this particular setup the grid size is 3x3 which is a 50% increase in the number of possible cell locations. The same level of increase is observed in the average error which is based upon the unity distance between adjacent cells. Furthermore, a fixed reader is used in this case with a more powerful antenna which might results in power leakage in a larger number of cells compared to the prior experiment.

5.4.2 Using Received Signal Strength Indicator(RSSI)

The results presented in the table 5.2 are obtained by using RSSI values only. We use the same hidden layer parameters as before. As before, the algorithm is run 100 times for all six folds for highest statistical significance and the average value is shown in the table. The last column describes the overall average error which is the averaged over six-folds. The results reported in this table for RSSI are worse than the ones reported above for TRC. The best localization performance is obtained at the same hidden layer size - however, the error is 1.33 which is larger than the unity error for adjacent cells. In fact, in a grid size of 3x3, a random guess of cell location results in an approximate error of 1.4 so the performance of the localization system is only slightly better than a random placement scheme. These results may indicate that RSSI by itself is not a reliable location indicator possibly due to susceptibility to noise and other factors.

Table 5.2 Location accuracy results using RSSI for different neural network topologies / augmented datasets and scenarios. Each scenario corresponds to a different phase of data collection process where: S1 - single tag with different orientations/antenna heights/power, S2 - single tag with metal object and S3 - one additional tag on the grid.

Hidden layer size	Samples	Total samples	Experiment	fold-1 error	fold-2 error	fold-3 error	fold-4 error	fold-5 error	fold-6 error	Average Error
[5 5]	216	216(54 x 4)	S1: RSSI	1.2652	1.1885	1.2061	1.1125	1.1084	1.4077	1.214733333
	324	540 (135 x 4)	S2: RSSI	0.6218	1.4728	1.3152	1.4194	1.7394	1.848	1.402766667
	324	864 (216 x 4)	S4: RSSI	1.3263	1.351	1.3582	1.3551	1.3183	1.3394	1.341383333
[10 10]	216	216(54 x 4)	S1: RSSI	1.1783	0.9884	1.034	0.9404	1.0346	1.319	1.08245
	324	540 (135 x 4)	S2: RSSI	0.6083	1.4447	1.2924	1.3753	1.823	1.9112	1.40915
	324	864 (216 x 4)	S4: RSSI	1.3578	1.3495	1.3422	1.3284	1.3366	1.3276	1.34035
5	216	216(54 x 4)	S1: RSSI	1.2483	1.1183	1.1038	1.0701	1.091	1.3727	1.167366667
	324	540 (135 x 4)	S2: RSSI	0.5987	1.445	1.2188	1.4129	1.8092	1.9283	1.40215
	324	864 (216 x 4)	S4: RSSI	1.3343	1.376	1.3293	1.3545	1.336	1.3326	1.343783333
10	216	216(54 x 4)	S1: RSSI	1.1902	1.0133	1.0536	0.9842	0.9999	1.289	1.088366667
	324	540 (135 x 4)	S2: RSSI	0.6167	1.4376	1.2566	1.3717	1.8237	1.9589	1.410866667
	324	864 (216 x 4)	S4: RSSI	1.3697	1.3253	1.3392	1.3387	1.3495	1.3564	1.346466667
20	216	216(54 x 4)	S1: RSSI	1.1158	0.9412	1.0686	0.9529	0.9094	1.2727	1.043433333
	324	540 (135 x 4)	S2: RSSI	0.6479	1.4411	1.2997	1.3619	1.8584	1.9571	1.427683333
	324	864 (216 x 4)	S4: RSSI	1.3166	1.3294	1.3314	1.3505	1.3434	1.3163	1.331266667

5.4.3 Using Tag Read Count(TRC) and Received Signal Strength Indicator(RSSI)

The results presented in the table 5.3 are obtained by combining the TRC and RSSI values using the same hidden layer size parameters as before. As before, the algorithm is run 100 times for all six folds for highest statistical significance and the average value is shown in the table. As can be seen from the table above, the prediction algorithm combining TRC and RSSI measurements provide significantly superior results compared to using each feature alone. Like the previous neural networks, the best performance is obtained at a hidden layer size of 20. In fact, the lowest localization error of 0.29 is achieved when the combined dataset is used for training and

testing. This is significantly lower than any of the prior experiments including the 2x3 grid setup and almost half the benchmark error of 0.5 (within-cell-accuracy).

Table 5.3 Location accuracy results using TRC and RSSI different neural network topologies / augmented datasets and scenarios. Each scenario corresponds to a different phase of data collection process where: S1 - single tag with different orientations/antenna heights/power, S2 - single tag with metal object, S3 - one additional tag on the grid and S4 - two additional tags on the grid.

Hidden layer size	Samples	total samples	Experiment	fold-1 error	fold-2 error	fold-3 error	fold-4 error	fold-5 error	fold-6 error	Average Error
[5 5]	432	432 (54 x 8)	S1 : TRC + RSSI	1.316	1.0981	1.1293	1.091	1.0781	1.4424	1.19258333
	648	1080 (135x8)	S2 : TRC + RSSI	0.667	1.3512	1.571	1.4484	1.8834	1.8455	1.46125
	648	1728 (216x8)	S4: TRC + RSSI	1.235	0.5556	0.268	0.2222	0.8698	0.4905	0.60701667
[10 10]	432	432 (54 x 8)	S1 : TRC + RSSI	1.204	0.8984	1.002	0.9943	0.8774	1.4483	1.07083333
	648	1080 (135x8)	S2 : TRC + RSSI	0.587	1.3154	1.531	1.4299	1.8811	1.9616	1.45115
	648	1728 (216x8)	S4: TRC + RSSI	1.661	0.6476	0.268	0.1111	0.3794	0.1571	0.53755
5	432	432 (54 x 8)	S1 : TRC + RSSI	1.163	0.8745	0.867	0.9162	0.7737	1.4528	1.008
	648	1080 (135x8)	S2 : TRC + RSSI	0.614	1.2995	1.515	1.431	1.8934	1.9622	1.45268333
	648	1728 (216x8)	S4: TRC + RSSI	0.692	0.4444	0.268	0.2682	0.2222	1.027	0.48715
10	432	432 (54 x 8)	S1 : TRC + RSSI	1.076	0.75	0.807	0.8661	0.659	1.4691	0.93811667
	648	1080 (135x8)	S2 : TRC + RSSI	0.526	1.2964	1.415	1.4086	1.9008	1.9875	1.42248333
	648	1728 (216x8)	S4: TRC + RSSI	0.831	0.4444	0.111	0.1571	0.4905	0.1111	0.35753333
20	432	432 (54 x 8)	S1 : TRC + RSSI	1.042	0.6351	0.806	0.8067	0.5977	1.4039	0.882
	648	1080 (135x8)	S2 : TRC + RSSI	0.504	1.2924	1.399	1.3898	1.8981	2.0104	1.41571667
	648	1728 (216x8)	S4: TRC + RSSI	0.738	0.4905	0	0	0.3794	0.1111	0.28665

CHAPTER 6: CONCLUSION AND FUTURE WORK

In this work we explored the potential of passive RFID systems for indoor localization by developing two grid-based experimental frameworks (symmetrical and asymmetrical) and using two standard and easily measurable performance metrics: received signal strength indicator (RSSI) and tag read count (TRC). Multiple scenarios were created to imitate real life challenges such as placing metal objects and other RFID tags in the read field. A neural network based prediction algorithm was used to analyze the localization accuracy when RSSI and TRC features where used both separately and together.

It was identified that the combination of both features provide the best prediction of cell location whereas TRC by itself could still provide reasonable localization in a grid-based setup. However, RSSI measurements by themselves proved to be susceptible to noise and other factors in the field resulting in subpar performance compared to using TRC or TRC + RSSI. Interestingly, while RSSI measurements alone performed almost similarly to random guessing of cell location, they worked to improve the performance of TRC features when combined due to enrichment of mutual information between these two feature sets.

Hidden layer size of the neural network also had an impact on performance as explained in the figure below. This graph below shows the plot of average error versus the hidden layer size. It can be observed that as the hidden layer size increases, the average error is reduced. From the graph, it is also clear that when compared one-on-one, TRC yield better indoor localization than RSSI for our particular experimental setup. The received signal strength Indicator(RSSI) metric is

susceptible to the presence of obstacles such as metal piece and other RFID tags in our experimental area. On the other hand, we can use the RSSI values along with TRC values to significantly improve the indoor localization. This is clearly seen in the Figure 6.1.

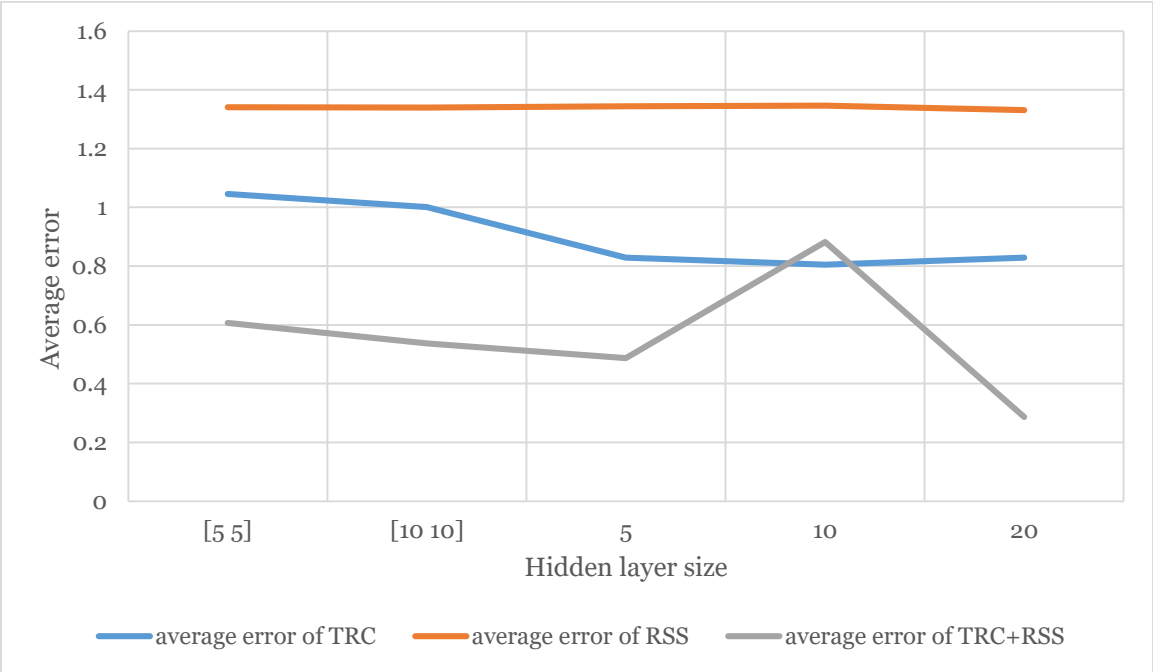

Figure 6.1 Comparison of hidden layer size and average error.

The Figure 6.2 shows the average errors for a set hidden layer size (20) for different datasets used in training. In the first data point, only the training data collected using a single tag is used. As one can see, when new data is introduced to the prediction algorithm by using the metal object, the performance of all three combinations (TRC, RSSI and TRC+RSSI) drop significantly. This is due to the novelty of introduced data for the neural network. This situation can be overcome by collecting more data as can be seen in the third section of the graph where additional measurements are added to the dataset in the form of two tag measurements which improve the performance of all three combinations. The biggest gains in localization accuracy is observed in the feature combination of TRC and RSSI - this is probably due to the fact that with

increasing dataset size, mutual information potential between these feature sets is also improved resulting in much reduced average errors compared to using TRC or RSSI alone.

Figure 6.2 Average errors for a set hidden layer size (20) for different datasets.

As future work, the grid area can be expanded to study the effects of distance on passive RFID tags. We can look into the analysis of the effects of neural network size and topology on localization performance. Run various competing algorithms such as triangulation and other data-driven approaches like regression to compare performance results with ANN. Also, we hope to explore the impact with change of the size and direction of data used in training the neural network on the localization performance. We will also explore expanding the feature set dimensions by including more antennas (in the fixed reader setup).

REFERENCES

[1] Siddhesh Doiphode, J W Bakal and Madhuri Gedam. Article: Survey of Indoor Positioning Measurements, Methods and Techniques. International Journal of Computer Applications 140(7):1-4, April 2016.

[2] J. R. Zhou, H. J. Zhang, H. L. Zhou, "Localization of Pallets in Warehouses Using Passive RFID System", *Journal of Central South University*, vol. 22, pp. 3017-3025, 2015.

[3] The Study on Using Passive RFID Tags for Indoor Positioning S.L. Ting, S.K. Kwok, Albert H.C. Tsang and George T.S. Ho Department of Industrial and Systems Engineering, The Hong Kong Polytechnic University, Hung Hom, Hong Kong, Hong Kong, China.

[4] M. Chan and X. Zhang, "Experiments for Leveled RFID Localization for Indoor Stationary Objects," *2014 11th International Conference on Information Technology: New Generations*, Las Vegas, NV, 2014, pp. 163-169.

[5] Hölzl, Michael & Neumeier, Roland & Ostermayer, Gerald. (2015). Localization in an Industrial Environment: A Case Study on the Difficulties for Positioning in a Harsh Environment. International Journal of Distributed Sensor Networks. 2015. 11. 10.1155/2015/567976.

[6] R. Melamed, "Indoor Localization: Challenges and Opportunities," *2016 IEEE/ACM International Conference on Mobile Software Engineering and Systems (MOBILESoft)*, Austin, TX, 2016, pp. 1-2.

[7] L. Vojtech, M. Nerada, J. Hrad and R. Bortel, "Outdoor localization technique using active RFID technology aimed for security and disaster management applications," *Proceedings of the 2015 16th International Carpathian Control Conference (ICCC)*, Szilvasvarad, 2015, pp. 586-589.

[8] A. Goetz, S. Zorn, R. Rose, G. Fischer and R. Weigel, "A time difference of arrival system architecture for GSM mobile phone localization in search and rescue scenarios," *2011 8th Workshop on Positioning, Navigation and Communication*, Dresden, 2011, pp. 24-27.

[9] J. Zhang, G. Han, N. Sun and L. Shu, "Path-Loss-Based Fingerprint Localization Approach for Location-Based Services in Indoor Environments," in *IEEE Access*, vol. 5, pp. 13756-13769, 2017.

[10] J. Zheng, T. Qin, J. Wu and L. Wan, "RFID indoor localization based on relational aggregation," *2016 Eighth International Conference on Advanced Computational Intelligence (ICACI)*, Chiang Mai, 2016, pp. 41-44.

[11] M. Bouet and A. L. dos Santos, "RFID tags: Positioning principles and localization techniques," 2008 1st IFIP Wireless Days, Dubai, 2008, pp. 1-5.

[12] H. Liu, H. Darabi, P. Banerjee and J. Liu, "Survey of Wireless Indoor Positioning Techniques and Systems," in IEEE Transactions on Systems, Man, and Cybernetics, Part C (Applications and Reviews), vol. 37, no. 6, pp. 1067-1080, Nov. 2007.

[13] M. Yassin and E. Rachid, "A survey of positioning techniques and location based services in wireless networks," 2015 IEEE International Conference on Signal Processing, Informatics, Communication and Energy Systems (SPICES), Kozhikode, 2015, pp. 1-5.

[14] L. Asmaa, K. A. Hatim and M. Abdelaaziz, "Localization algorithms research in wireless sensor network based on Multilateration and Trilateration techniques," 2014 Third IEEE International Colloquium in Information Science and Technology (CIST), Tetouan, 2014, pp. 415-419.

[15] Z. Belhadi, L. Fergani, B. Fergani and J. M. Laheurte, "RFID tag indoor localization by Fingerprinting methods," *2014 4th International Conference on Wireless Communications, Vehicular Technology, Information Theory and Aerospace & Electronic Systems (VITAE)*, Aalborg, 2014, pp. 1-5.

[16] S. R. Borra, G. J. Reddy and E. S. Reddy, "A broad survey on fingerprint recognition systems," *2016 International Conference on Wireless Communications, Signal Processing and Networking (WiSPNET)*, Chennai, 2016, pp.1428-1434.

[17] Wikipedia contributors. "Pattern recognition." *Wikipedia, The Free Encyclopedia*. Wikipedia, The Free Encyclopedia, 13 Sep. 2017. Web. 24 Oct. 2017.

[18] T. H. Dao, M. T. Le and Q. C. Nguyen, "Indoor localization system using passive UHF RFID tag and multi-antennas," *2014 International Conference on Advanced Technologies for Communications (ATC 2014)*, Hanoi, 2014, pp. 405-410.

[19] T. H. Dao, Q. C. Nguyen, V. D. Ngo, M. T. Le and C. A. Hoang, "Indoor Localization System Based on Passive RFID Tags," *2014 5th International Conference on Intelligent Systems, Modelling and Simulation*, Langkawi, 2014, pp. 579-584.

[20] http://pages.cs.wisc.edu/~bolo/shipyard/neural/local.html, University of Wisconsin-Madison, Computer Sciences User Pages, 2015.

[21] B. Cheng, R. Du, B. Yang, W. Yu, C. Chen and X. Guan, "An Accurate GPS-Based Localization in Wireless Sensor Networks: A GM-WLS Method," *2011 40th International Conference on Parallel Processing Workshops*, Taipei City, 2011, pp. 33-41.

[22] W. Vinicchayakul, S. Promwong and P. Supanakoon, "Study of UWB indoor localization using fingerprinting technique with different number of antennas," *2016 International Computer Science and Engineering Conference (ICSEC)*, Chiang Mai, 2016, pp. 1-4.

[23] M. Liu *et al*., "RFID indoor localization system for tag and tagfree target based on interference," *2017 19th International Conference on Advanced Communication Technology (ICACT)*, Bongpyeong, 2017, pp. 372-376.

[24] Park, C.R.; Eom, K.H. RFID Label Tag Design for Metallic Surface Environments. *Sensors* 2011, *11*, 938-948.

[25] https://www.doc.ic.ac.uk/~nd/surprise_96/journal/vol4/cs11/report.html, Neural Networks, C Stergiou and D Siganos, Imperial College London, 2017.

[26] doug (https://stats.stackexchange.com/users/438/doug), How to choose the number of hidden layers and nodes in a feedforward neural network?, 2017.